Title

Resonant cavity based time-domain multiplexing techniques for coherently combined fiber laser systems

Journal

The European Physical Journal Special Topics, 224(13)

ISSN

1155-4339

Authors

Zhou, T
Ruppe, J
Stanfield, P
et al.

Publication Date

2015-10-01

DOI

10.1140/epjst/e2015-02569-5

Peer reviewed

Eur. Phys. J. Special Topics **224**, 2585–2602 (2015)

DOI: 10.1140/epjst/e2015-02569-5

THE EUROPEAN PHYSICAL JOURNAL SPECIAL TOPICS

Regular Article

Resonant cavity based time-domain multiplexing techniques for coherently combined fiber laser systems

T. Zhou[1,a], J. Ruppe[1], P. Stanfield[1], J. Nees[1], R. Wilcox[2], and A. Galvanauskas[1]

[1] Center for Ultrafast Optical Science, University of Michigan, Ann Arbor, MI 48109, USA
[2] Lawrence Berkeley National Laboratory,1 Cyclotron Road, Berkeley, CA 94720, USA

Received 5 June 2015 / Received in final form 31 August 2015
Published online 26 October 2015

Abstract. This paper describes novel time-domain multiplexing techniques that use various resonant cavity configurations for increasing pulse energy extraction per each parallel amplification channel of a coherently combined array. Two different techniques are presented: a so-called N^2 coherent array combining technique, applicable to a periodic pulse train, and a coherent pulse stacking amplification (CPSA) technique, applicable to a pulse burst. The first technique is a coherent combining technique, which achieves simultaneous beam combining and time-domain pulse multiplexing/down-counting using traveling-wave Fabry-Perot type resonators. The second technique is purely a time-domain pulse multiplexing technique, used with either a single amplifier or an amplifier array, which uses traveling-wave Gires-Tourmois type resonators.

The importance of these techniques is that they can enable stacking of very large number of pulses, thus increasing effective amplified-pulse duration potentially by 10^2 to 10^3 times, and reducing fiber array size by the corresponding factor. This could lead to very compact coherently combined arrays even for generating very high pulse energies in the range of 1 to 100 J.

1 Introduction

Achieving very-high-energy short pulses from fiber amplifier systems is practically hindered by peak power limitations due to detrimental nonlinear effects, such as self-phase modulation, four-wave-mixing, critical self-focusing, etc. The chirped pulse amplification (CPA) technique alleviates this limitation by a factor of up to 10^3–10^4 times by stretching broadband ultrashort pulses prior to amplification and compressing them afterwards [1], thus enabling pulse energies up to the range of 100 μJ to $\sim$1 mJ, which is yet much less than the stored pulse energy of the fiber amplifier [2].

[a] e-mail: tongzhou@umich.edu

Consequentially, achieving approximately 40 J per ultrashort pulse as needed for a 10 GeV laser-plasma acceleration stage [3], would require combining of 10^4–10^5 parallel amplification channels in a coherently phased fiber laser array. There is a significant room for improvement in achievable pulse energies per channel, provided that all stored energy in a fiber could be fully extracted. To achieve that one needs to amplify much longer pulses than are obtainable in a CPA approach. As a step in this direction a divided pulse amplification (DPA) technique has been proposed recently [4,5], which is based on pre-amplification spatial pulse-splitting and post-amplification pulse-recombining. However, since it requires delay lines whose lengths increase exponentially with the number of pulse division stages, DPA technique appears to be limited to a relatively small number of pulses (approximately 10). Coherent pulse stacking and dumping techniques have also been proposed recently, in which stored stacked pulses in a high-finesse resonant enhancement cavity are dumped out using an active cavity-dumping element, e.g. an acousto-optic modulator (AOM) [6], or a rotating-mirror [7]. However, this technique faces significant pulse energy limitations when an intra-cavity dumping is done with any available electro-optical or acousto-optical modulator technology, and the precision and stability constrains when the cavity dumping can be performed using mechanical rotating-mirror arrangement.

To maximize achievable pulse energy per CPA channel, in this paper a class of time-domain pulse synthesis techniques is proposed, consisting of periodic-pulse N^2 coherent combining, and coherent pulse stacking amplification (CPSA) [8] methods. Both proposed techniques use passive resonant cavities without any intra-cavity components as their combiner/stacker at the system output, and control pulse stacking/beam combining at the front-end of the system through amplitude and phase modulation imprinted directly onto a periodic-pulse seed from a mode-locked laser oscillator. The distinct advantages of this class of techniques are the following: (1) The use of resonator cavities instead of delay lines results in small-footprint arrangements, (2) absence of intra-cavity components eliminates the modulator-induced pulse energy limit and the complexity of incorporating mechanical rotating-mirrors; (3) By modulating the pulse sequence directly from a mode-locked oscillator, this class of proposed techniques does not require any initial pulse splitting or stretching, which can be integrated in a monolithic circuitry when built using fiber optics. The modulation prior to major amplification also allows the generation of any arbitrary temporal profile of individual pulses and of the overall pulse sequence, thus can be used to pre-compensate saturation and nonlinear effects in the amplifiers even at maximum pulse energies.

In this class of proposed techniques, N^2 coherent combining represents coherent pulse synthesis in both time and spatial domains, enhancing both average power and pulse energy. Average power is increased proportionally to the number of channels N in an array, the same as in any other coherent or incoherent combining approaches. The unique aspect of N^2 combining is that it simultaneously reduces by N times pulse repetition rate in the combined beam at the system output, thus increasing the resulting energy per pulse proportionally to N^2 times. On the other hand, coherent pulse stacking amplification (CPSA) implements coherent pulse synthesis purely in time domain, by stacking a burst of input pulses into a single output pulse, and can therefore be used with either an amplifier array or a single amplifier. Use of these techniques enables achieving high pulse energies with relatively small number of parallel coherently-phased amplification channels, much smaller than would be required by using conventional coherently combined arrays.

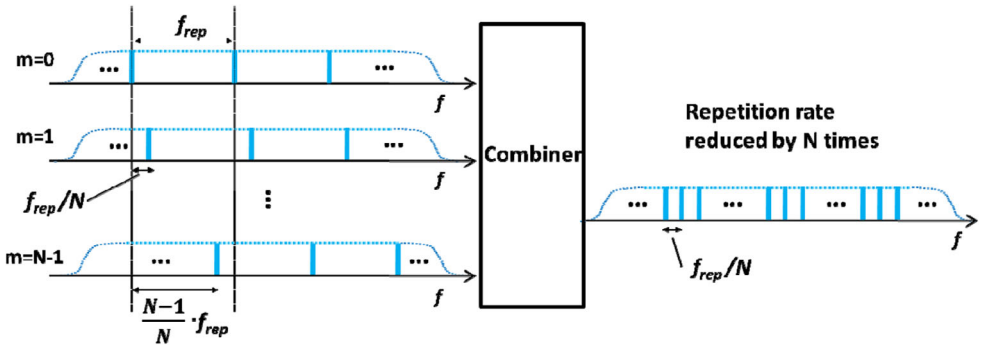

Fig. 1. The concept of N^2 coherent combining.

2 N^2 coherent combining

2.1 Concept of N^2 coherent combining

Figure 1 outlines the concept of N^2 coherent combining, showing how N spatially-separate periodic pulse trains (in parallel channels labeled $m = 0, 1, \ldots, N-1$) can be combined into one spatial beam with N-times lower pulse repetition rate. The concept can be best explained in frequency domain. N^2 combining can only be achieved with strictly periodic pulse trains. In frequency domain such signals are described by a pulse envelope, multiplied by a frequency-comb (i.e. a frequency-periodic sequence of vanishingly-narrow spectral lines). The separation between frequency-comb lines corresponds to the pulse repetition frequency f_{rep}. In this arrangement all parallel channels have the same repetition frequency and the same pulse envelope. However, for achieving N^2 combining it is necessary that each-channel signal is individually phase modulated such that the m-th channel frequency comb is frequency shifted by $(m/N) \cdot f_{\mathrm{rep}}$ with respect to the m = 0 channel signal. Then linear addition in a combiner of all N evenly shifted frequency combs should produce a signal, which in spectral domain is characterized by the same pulse envelope, but with N times denser frequency comb lines separated by f_{rep}/N. In time domain this corresponds to N times lower pulse repetition rate compared to the repetition rate in each of the channels. Consequentially, since average power in the combined beam is approximately N times higher, and the pulse repetition rate is N times lower than those of each channel, the combined-signal pulse energy is approximately N^2 times higher than in each channel.

Such a linear addition of beams containing evenly shifted frequency-combs can be achieved using beam combiners based on Fabry-Perot interferometer (FPI) cavities. This is shown in Fig. 2, where the simplest case of two-beam combining is presented as an illustrative example. Such two-beam combining requires a single FPI cavity, which in Fig. 2(a) is represented by a traveling-wave configuration consisting of partially reflecting front mirrors with reflectivity $\mathrm{R_F} < 1$, and fully reflecting folding mirrors with $\mathrm{R_b} = 1$. Fabry-Perot spectral transfer functions for reflection R(f) and transmission T(f) (shown in Fig. 2(b)) are:

$$R(f) = \frac{\sqrt{R_F} \cdot (1 - e^{i2\pi f\delta/c})}{1 - R_F \cdot e^{i2\pi f\delta/c}} \quad \text{and} \quad T(f) = \frac{e^{i\pi f\delta/c} \cdot (1 - R_F)}{1 - R_F \cdot e^{i2\pi f\delta/c}}. \tag{1}$$

Here δ is the cavity round trip length, and c is the speed of light in the cavity. If the FPI round-trip time is equal to the pulse repetition period, then the cavity's free spectral range $\Delta f_{FSR} = c/\delta$ is equal to the pulse repetition rate f_{rep}. Consequentially, such

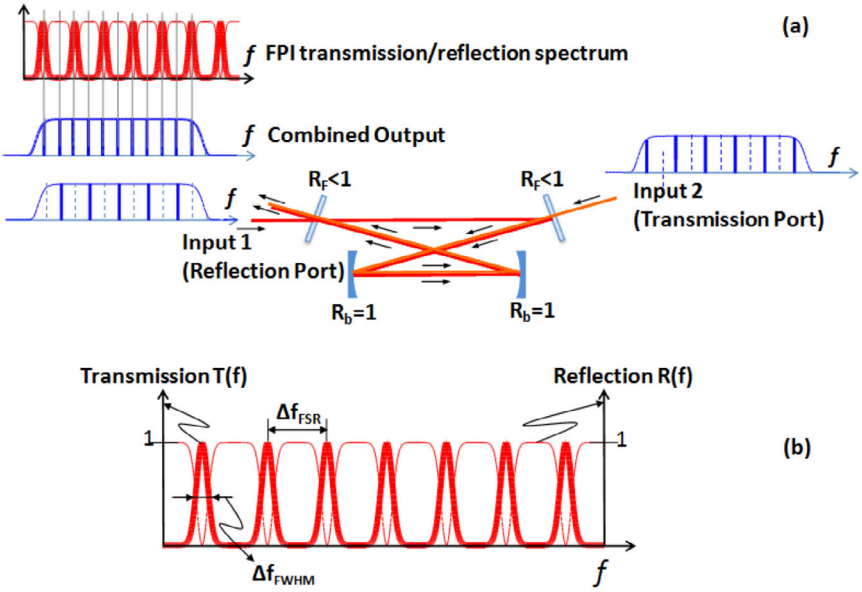

Fig. 2. N^2 coherent combining with a single cavity.

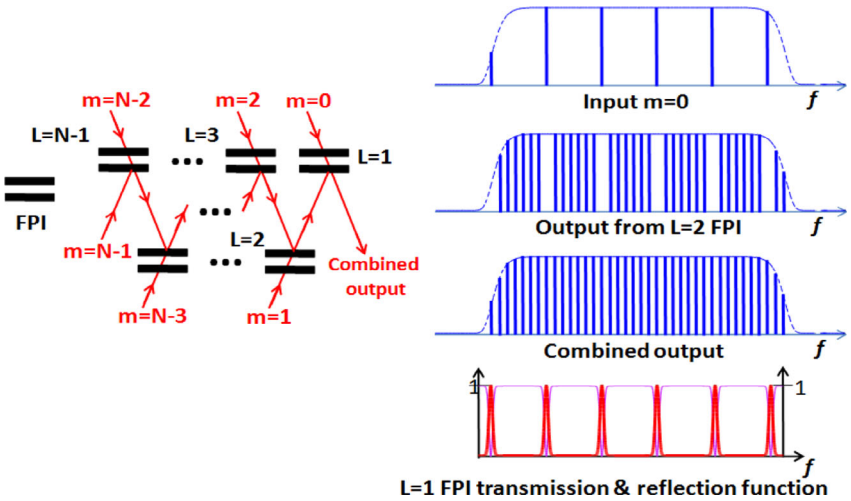

Fig. 3. A FPI sequence arrangement for N^2 coherent combining of N parallel channels.

a cavity can act as an optical signal inter-leaver for the two evenly-shifted frequency combs, provided that cavity roundtrip δ is suitably selected to center transmission and reflection channel spectral transfer functions on the corresponding frequency combs, as shown in Fig. 2(a). This means that it is necessary to stabilize cavity length to the required length δ, as discussed in more detail in Sect. 2.4.

For combining more than two beams, it is necessary to use more than one FPI cavity. Figure 3 shows an example of an FPI arrangement for coherent combining of N parallel channels, consisting of N-1 FPI cavities arranged sequentially. In this case it is important to note that each cavity should have its finesse (i.e. ratio between FPI free spectral range and its transmission linewidth $\Delta f_{FSR}/\Delta f_{FWHM} = \pi\sqrt{F}/2$, where $F = 4R_F/(1-R_F)^2$) at least equal to the number of combined channels

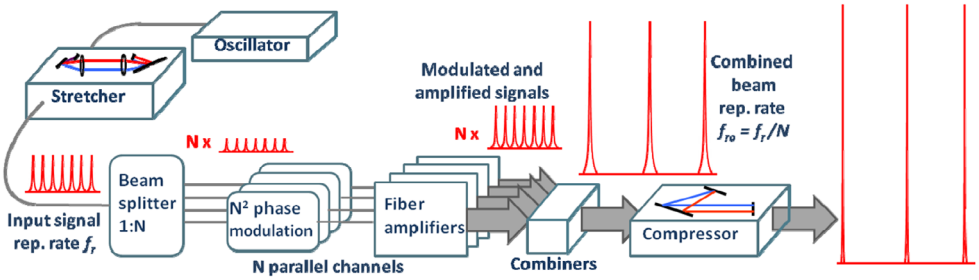

Fig. 4. The architecture of a N^2 coherent combining system.

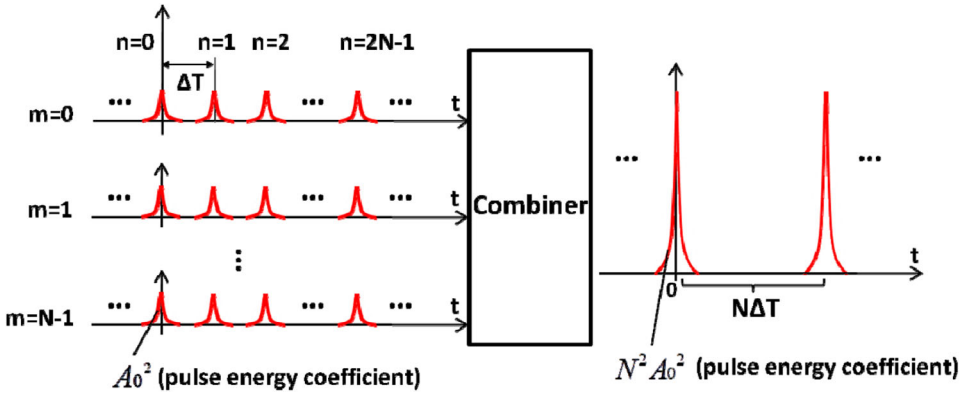

Fig. 5. Time-domain picture of N^2 coherent combining showing the input and output pulse sequences as well as their pulse energy coefficients.

$\Delta f_{FSR}/\Delta f_{FWHM} \geq N$. Furthermore, each cavity's round-trip length δ_L should be individually selected (and stabilized) to align its transmission peak with the frequency comb of the corresponding transmitting input signal.

Overall N^2 system architecture for a fiber CPA array is shown in Fig. 4. In this system initial seed of periodic pulses at f_{rep} from a mode-locked oscillator is split into N parallel amplification channels, where each signal can be frequency shifted by applying a suitably selected linear phase ramp through a phase modulator in each parallel channel. Note that such phase modulation would be relatively slow, since it is determined by the repetition rate f_{rep}. Since typical f_{rep} for mode-locked sources are in ~100 MHz range, this should be easily achievable with standard 10 GHz telecom-grade electro-optic modulators.

2.2 Time-domain analysis of N^2 coherent combining

Figure 5 shows the time-domain picture of N^2 coherent combining, where it is assumed that all pulses at the input and output have identical complex envelopes $\tilde{p}_s(t)$. The complex notation accounts for the fact that stacking can be achieved with bandwidth-limited (described by real envelopes $\widetilde{p}_s(t) \equiv p_s(t)$) as well as with chirped (described by complex envelopes $\tilde{p}_s(t)$) pulses. The time axis reference is set in a way such that the 0-th pulses in all the input channels are centered at t = 0. It is also assumed that all the input channels have identical pulse amplitude A_0 and identical pulse repetition period ΔT. In addition, to achieved N^2 coherent combining, a specific phase

code/modulation (which shifts the frequency combs of the input pulse sequences as discussed in Sect. 2.1) is applied to the input pulse sequences, e.g. the n-th pulse in the m-th channel is phase modulated with a phase shift:

$$\psi_{mn} = e^{in\frac{m}{N}2\pi}. \tag{2}$$

Thus this pulse can be expressed as

$$\tilde{p}_{mn}(t) = A_0 e^{in\frac{m}{N}2\pi} \cdot \tilde{p}_S(t - n\Delta T) e^{i\omega_0(t-n\Delta T+\phi_{0mn})}, \tag{3}$$

where ω_0 is the pulse carrier angular frequency and φ_{0mn} is the carrier initial phase. To achieve N^2 coherent combining, φ_{0mn} needs to be synchronized so that

$$\phi_{0mn} = \phi_{0n}, \tag{4}$$

which corresponds to the phase locking discussed in Sect. 2.4. Thus the combined n-th pulse can be derived as

$${}^{out}\tilde{p}_n(t) = \sum_{m=0}^{N-1} \tilde{p}_{mn}(t) = A_0 \cdot \tilde{p}_S(t - n\Delta T) e^{i\omega_0(t-n\Delta T+\phi_{0n})} \sum_{m=0}^{N-1} e^{im\frac{n}{N}2\pi}. \tag{5}$$

Since mathematically we have $\sum_{m=0}^{N-1} e^{im\frac{n}{N}2\pi} = 0$ if $\frac{n}{N}$ is not an integer, we get

$$\begin{cases} {}^{out}\tilde{p}_n(t) = 0, & \text{when } \dfrac{n}{N} \text{ is not an integer} \\ {}^{out}\tilde{p}_n(t) = NA_0 \cdot \tilde{p}_S(t - n\Delta T) e^{i\omega_0(t-n\Delta T+\phi_{0n})}, & \text{when } \dfrac{n}{N} \text{ is an integer} \end{cases} \tag{6}$$

$$\begin{cases} {}^{out}A_n = 0,\ {}^{out}B_n = 0, & \text{when } \dfrac{n}{N} \text{ is not an integer} \\ {}^{out}A_n = NA_0,\ {}^{out}B_n = N^2A_0^2, & \text{when } \dfrac{n}{N} \text{ is an integer} \end{cases}, \tag{7}$$

where ${}^{out}A_n$ is the amplitude of the combined n-th output pulse, and ${}^{out}B_n$ is the corresponding pulse energy coefficient of the combined n-th output pulse ${}^{out}B_n = |{}^{out}A_n|^2$. Thus a repetition-rate down-counting factor of N and a combined pulse energy enhancement factor of N^2 are shown.

2.3 Experimental demonstration of N^2 coherent combining

The system layout of the 2-channel N^2 coherent combining experiment is shown in Fig. 6. The system consists of a mode-locked laser, a grating stretcher, two parallel fiber amplifier channels, a FPI based combiner, and a grating compressor. It also contains the control electronics for coherent phasing of the parallel fiber amplifier channels, as well as cavity-length stabilization of the FPI combiner.

The mode-locked laser operates at a central wavelength of 1059 nm, a repetition rate of 72 MHz, a spectral width of 12 nm, and an output power of 100 mW. The diffraction-grating based pulse stretcher is arranged in a standard Martinez-type configuration, and it stretches output pulses from the mode-locked oscillator to a pulse width of ∼900 ps. The stretched pulse sequence is then modulated by a free-space acousto-optic modulator (AOM), so that the pulse repetition rate can be down-counted for achieving optimized fiber amplifier performances. The pulse sequence is afterwards coupled into polarization maintaining (PM) single-mode fiber (SMF), and amplified by two SMF pre-amplifiers before splitting into two parallel

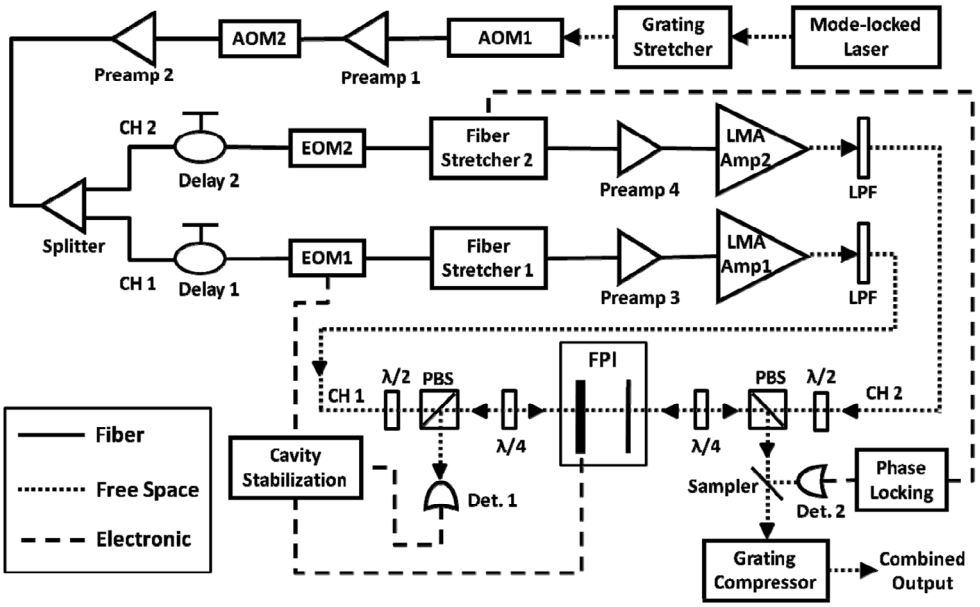

Fig. 6. Experimental N^2 coherent combining system. CH1/2: Channel 1/2; Preamp: pre-amplifier; LMA Amp.: large-mode-area fiber amplifier; LPF: long(wavelength)-pass filter; $\lambda/2$: half-wave plate; $\lambda/4$: quarter-wave plate; FPI: Fabry–Perot interferometer; Det.: detector.

fiber amplifier channels. Amplification in each of the two SMF pre-amplifier stages is implemented using standard in-core pumped Yb-doped PM SMF and a standard telecom-grade single-mode pump diode. A monolithic AOM is inserted between the two pre-amplifiers, serving as an optical gate to suppress the unwanted amplified spontaneous emission (ASE) background between pulses. It also can be used to additionally down-count the pulse repetition rate for optimizing amplifier performances.

The pre-amplified pulse sequence is then split into two parallel fiber amplifier channels with a 50:50 single-mode fiber splitter. Parallel amplification channels consist of identical components with identical fiber lengths to ensure that each optical path is of equal length and with equal amount of linear and higher-order dispersion. In each parallel amplifier channel, the pulse sequence goes through a delay line, an electro-optic modulator (EOM), a fiber stretcher, a SMF pre-amplifier, and a large-mode-area (LMA) fiber amplifier before being coupled out. A compact precise adjustable delay line is used in each amplifier channel to achieve optical-path matching. The fiber-coupled electro-optic (EO) lithium niobate (LiNbO3) phase modulator EOM 1 in Channel 1 (CH1) is driven by the cavity-stabilization electronics to apply a frequency modulation to the CH1 pulse sequence, which is required for actively stabilizing the cavity length of the Fabry–Perot interferometer (FPI) combiner (discussed in Sect. 2.4). Meanwhile EOM 2 in Channel 2 (CH2) applies the required N^2 phase modulation/code to the CH2 pulse sequence. The piezoelectric fiber stretcher based phase modulator in CH2 is used for correcting the phase drift between the two amplifier channels, which will be shown in Sect. 2.4. In each amplifier channel, the pulse sequence is further amplified by a SMF pre-amplifier and a subsequent co-pumped 25 μm large-mode-area (LMA) fiber amplifier. After the pulse sequence is coupled out from each amplifier channel, a long-pass filter (LPF) with its cutting-off wavelength tuned to 1045 nm is implemented to filter out the ASE background in the amplified signal.

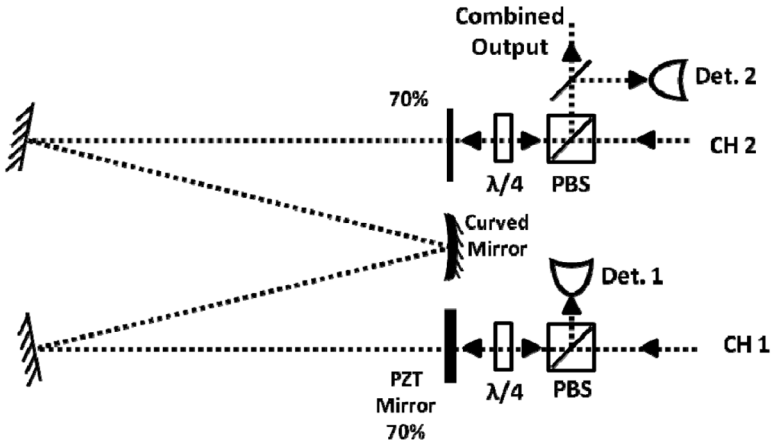

Fig. 7. The combiner part of the N^2 coherent combining setup. CH1/2: Channel 1/2; $\lambda/2$: half-wave plate; $\lambda/4$: quarter-wave plate; Det.: detector.

Figure 7 shows the combiner part of the N^2 coherent combining setup, which includes a 5-mirror FPI cavity, two quarter waveplates, and two polarized beam splitters (PBS). The FPI cavity consists of two flat highly reflective mirrors (R = 99.5%), a curved highly reflective mirror (R = 99.5%), and two flat partially reflective cavity mirrors (R = 70%). Here a curved mirror is implemented to make the FPI cavity q-preserving for better interferences at the partially reflective cavity mirrors. Two pulse sequences from CH1 and CH2 are incident to the FPI cavity from opposite sides of the cavity. A set of PBS and quarter waveplate is implemented on each side of the FPI cavity for beam guidance while ensuring the same polarization for the two channels to interfere. The interference between the cavity transmission signal of CH1 and the cavity reflection signal of CH2 makes the combined output signal, and a small fraction of it is monitored by detector 2 for phase locking between the two channels. Meanwhile the output signal from the other side of the cavity is monitored by detector 1 for FPI cavity length stabilization. Both phase locking and cavity stabilization are required for N^2 coherent combining and will be discussed in Sect. 2.4. Finally the combined output pulse sequence is launched into a standard Treacy-type diffraction grating compressor.

2.4 System requirements for N^2 coherent combining

In this N^2 coherent combining experiment, the N^2 phase code is applied to the pulse sequence in CH2 through EOM2, so that every other pulse in the sequence is applied a π phase shift according to Eq. (2). In frequency domain, this phase modulation shifts the frequency comb of the CH2 signal by half the repetition rate. Both the time domain and frequency domain pictures are shown in Fig. 8.

From the discussion in Sect. 2.1, the FPI cavity length needs to be stabilized such that the free spectral range of the FPI cavity should be the same as the repetition rate of the input pulse sequences, the transmission peaks of the FPI transfer function should be aligned with the frequency comb of the CH1 signal, and the rejection band centers should be aligned with the frequency comb of the CH2 signal. Here we develop a cavity stabilization scheme in the presence of both channel inputs, which is done by using Det. 1 to monitor the total average power signal ($S_{\mathbf{cs}}$) of the cavity transmission signal of CH2 and the cavity reflection signal of CH1. The simulation present in Fig. 9

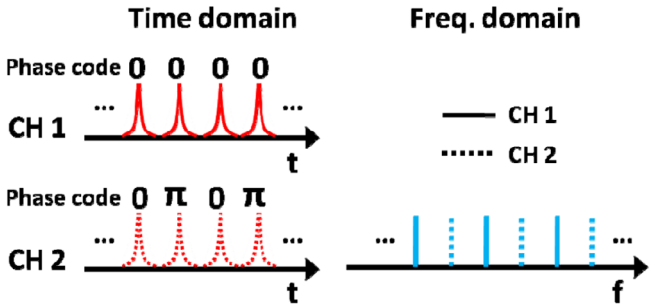

Fig. 8. The time domain and frequency domain pictures of the two input pulse sequences with the N^2 phase code.

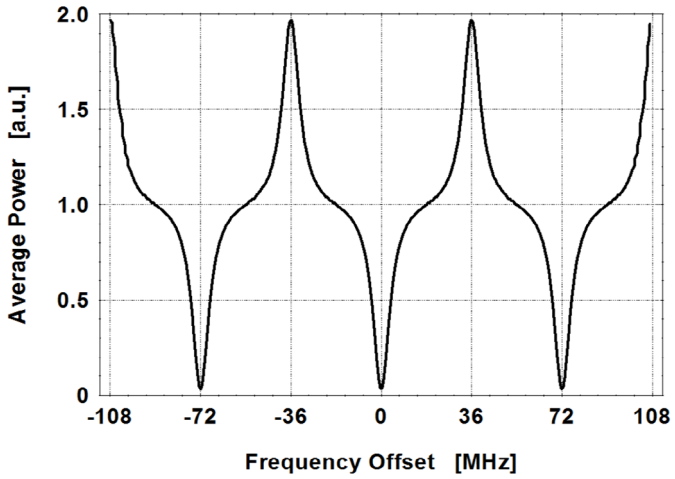

Fig. 9. The total average power signal $\boldsymbol{S}_{\mathbf{cs}}$ on Det. 1 versus the frequency offset between the FPI transmission peaks and the frequency comb components of the pulse sequence in CH1.

shows the total average power signal $\boldsymbol{S}_{\mathbf{cs}}$ on Det. 1 versus the frequency offset between the FPI transmission peaks and the frequency comb components of the pulse sequence in CH1, where the required cavity stabilization is achieved when the frequency offset vanishes. This is done by electronically minimizing the Det. 1 signal $\boldsymbol{S}_{\mathbf{cs}}$, which in details is done by applying a ∼2 MHz frequency modulation to EOM1, monitoring and demodulating the total average power signal $\boldsymbol{S}_{\mathbf{cs}}$, and applying a proper feedback signal to drive the PZT cavity mirror after a series of signal processing.

To achieve perfect interferences of the pulse sequences from different channels on the FPI cavity mirror, both group delay matching and pulse phase synchronization need to be satisfied. Accurate matching of the group delays between parallel channels is required so that the pulses are exactly overlapped in time when interfering. In practice, acceptable group-delay errors should be much smaller than the pulse duration, and for femtosecond pulses should be on the order of few micrometers. As shown in Fig. 7, the combining interferences happen on the non-PZT cavity mirror, thus the pulse sequences from CH1 and CH2 should travel the same optical path upon arrival at that mirror, which means prior to the FPI cavity CH2 should have an optical path which is longer than that of CH1 by a cavity single trip. Besides, the adjustable delay line in each channel is used to fine tune the optical path in micrometer precision to match the group delay of the two channels.

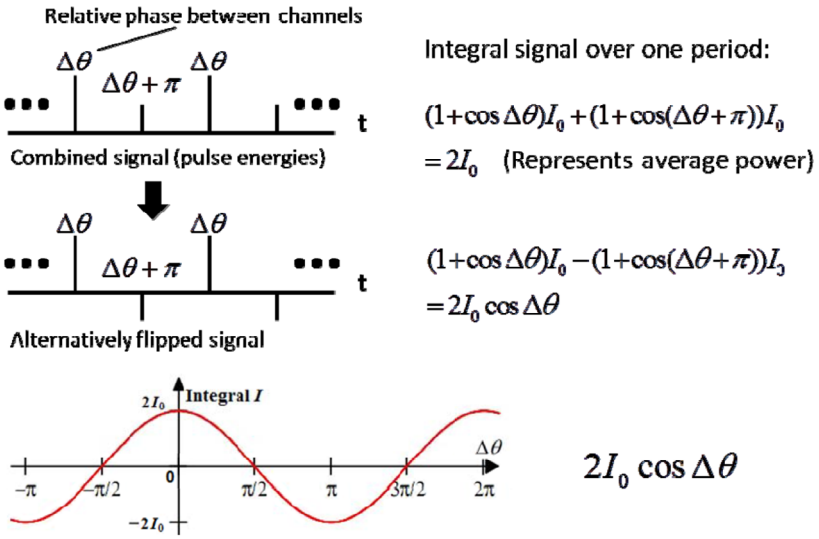

Fig. 10. Creating a phase-dependent integral signal for phase locking in N^2 coherent combining. Here I_0 is a constant integral value.

According to Eq. (4), to achieve N^2 coherent combining the carrier initial phases of all channels should be synchronized. For this 2-channel experiment, every other unmodulated pulse in the CH2 pulse sequence should be in phase with the CH1 pulse upon interference. Unlike the case of phase locking in conventional coherent beam combining of short pulses [9], in this experiment the average power of the combined output signal does not depend on the relative phase between the two channels, which is shown in Fig. 10. Here we developed a phase locking scheme for N^2 coherent combining by electronically flipping every other combined pulse in the combined sequence by mixing it with a square wave whose frequency is half the repetition rate of the input pulse sequences, integrating the flipped combined pulse signal with a proper filter, thus creating a phase-dependent integral signal for phase locking. This process is shown in Fig. 10, where it is clear that the required phase locking can be achieved by maximizing the phase-dependent integral signal I, which is done by applying a phase modulation to fiber stretcher 2, monitoring and demodulating the average power signal of a fraction of the combined output signal, and applying a proper feedback signal back to drive fiber stretcher 2 after a series of signal processing.

2.5 Experiment results and analysis

After the N^2 phase code is applied to the pulse sequence in CH2 (shown in Fig. 8) and the group delays of the two channels are matched, Det. 2 monitors the combined pulse sequence, as well as the FPI output for each individual input channel when the other channel is blocked, which are all shown in Fig. 11. Here the pulse sequences from individual channels are recorded without stabilizing the FPI cavity since in this experiment cavity stabilization is achieved with the presence of both channel inputs. Instead they are captured as their maximums received by Det. 2, since cavity stabilization maximizes those signals received by Det. 2. The combined pulse sequence is recorded after the cavity is stabilized and the phases of the pulse sequences from the two channels are synchronized.

From the data shown in Fig. 11, the pulse energy enhancement factor is measured to be ∼3.5, which is defined as the peak power ratio between the combined pulses

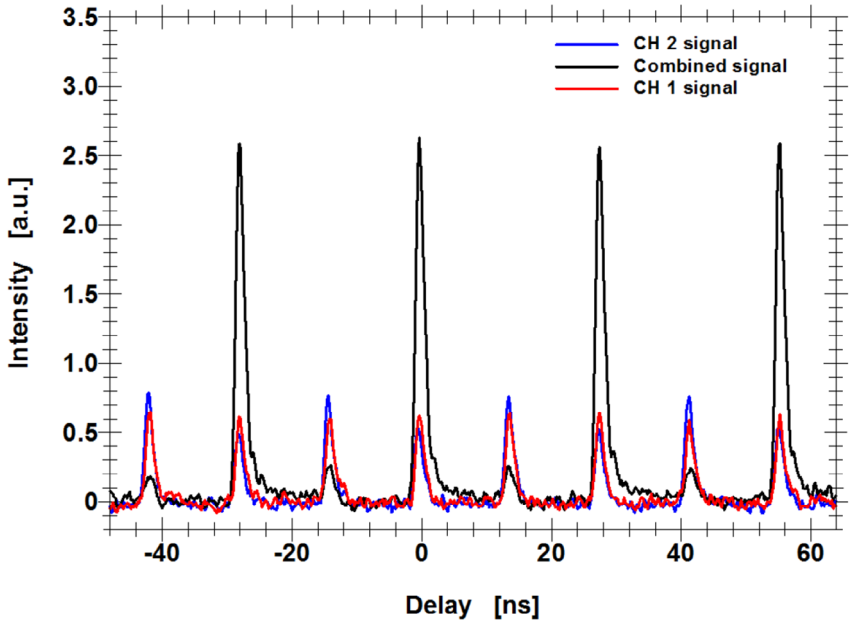

Fig. 11. The output coherently combined signal and the FPI output signal for each individual input channel (when the other channel is blocked).

and the most intense pulses from individual channels. The combining contrast is measured to be 10.6 dB, which is defined as the peak power ratio between the combined pulses and the residual pulses in the combined pulse sequence. Here the pulse energy enhancement factor is smaller than theoretical 4, and the combining contrast is limited. The main contributing factor was the amplitude modulation in the FPI output signal for CH2, introduced by an imperfect N^2 phase modulation as well as an offset between the stabilized FPI transfer function and the input frequency comb.

Since cavity mirrors with a 70% reflectivity are used in this experiment, when the required cavity stabilization is achieved the FPI transmission for the CH1 pulse sequence should be around 100%, while the FPI reflection for the CH2 pulse sequence should be around 97%. As a result, the absolute pulse energy enhancement factor, which is defined as the peak power ratio between the combined pulses and the most intense input pulses to the FPI combiner, should be around 97% of the measured pulse energy enhancement factor of 3.5, which is 3.4.

3 Coherent pulse stacking amplification (CPSA)

3.1 CPSA technique

Coherent pulse stacking amplification (CPSA) is a time-domain pulse multiplexing technique based on passive low-finesse Gires-Tournois interferometers (GTI), where a burst of amplitude and phase modulated input pulses are coherently stacked into a solitary output pulse. Unlike N^2 combining, there is only one input beam into a GTI cavity stacker, containing a burst of equal amplitude pulses in the time domain, and producing a solitary pulse at the output. By utilizing few GTI cavities (5-15), this technique gives the ability to stack up to 10–10^3 equal amplitude pulses from a

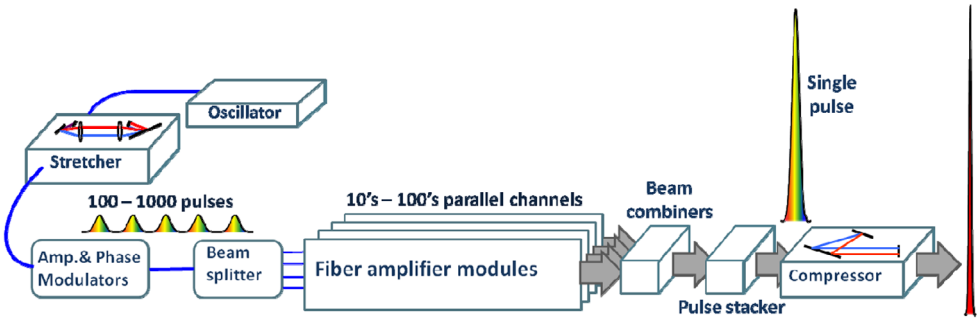

Fig. 12. Spatial multiplexing and time multiplexing system for generating >10 J pulse energy at >100 kW average power.

burst into a single pulse that contains the energy of the entire burst. This allows the extraction of all of the energy stored in a fiber amplifier, in the range of 10 mJ to 50 mJ, with negligible nonlinear effects.

CPSA can be used either with a single fiber amplifier, or it can be used with an array of fiber amplifiers, where the output from the array is first spatially combined using conventional methods, and then the output from the spatial combiner is sent into the GTI stackers where the pulse burst is transformed into a single pulse. Thus by using multiple GTIs in conjunction with spatial combining of parallel channels, output pulse energies in the range of >100 mJ to >10 J can be obtained by extracting all of the stored energy from >10 to >100 of parallel channels as shown in Fig. 12. This gives a path for generating pulses in the 10 J range at high repetition rates of >10 kHz, thus giving average powers at >100 kW. Additionally low input pulse energies reduce nonlinear effects so that they are negligible and have little impact on the stacking, combining, and compression at the output.

It is beneficial to first discuss the working principle of CPSA with a single GTI as well as its maximum enhancement limit before moving on to the more complicated, but also far more useful, case of using multiple GTIs to obtain very large enhancement factors.

3.2 CPSA with a single GTI

As illustrated in Fig. 13, CPSA with a single GTI operates so that all of the pulses in a pulse burst prior to the final pulse interfere destructively at the partially-reflecting cavity front mirror, thus storing all of their energy in the cavity, until the final pulse in the burst arrives and interferes constructively with the intra-cavity pulse at the cavity front mirror, thereby switching out all of the pulse energy stored in the cavity. During the stacking process, the cavity roundtrip length must be properly stabilized in order to achieve the desired interferences. In this single cavity configuration our analysis shows that the pulse energy enhancement, which is defined as the ratio between the pulse energy of the stacked output pulse and the highest pulse energy in the incident pulse burst input to the GTI stacker, depends on the reflectivity of the partially-reflecting cavity front mirror, and is optimum when the reflectivity is ∼40% [8]. The corresponding pulse energy enhancement is ∼2.5. A CPSA simulation based on a single GTI cavity with 5 input pulses and a front mirror reflectivity of R = 38.2% is presented in Fig. 14, showing an input pulse burst and the output stacked pulse, with a numerical pulse energy enhancement factor of 2.62. Note here

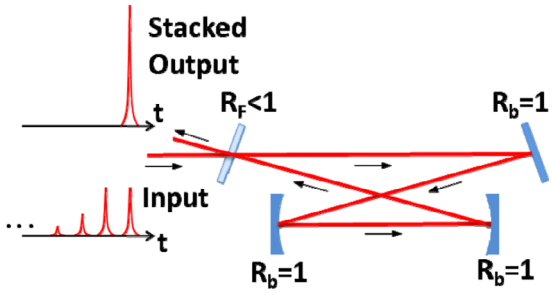

Fig. 13. CPSA with a single GTI cavity.

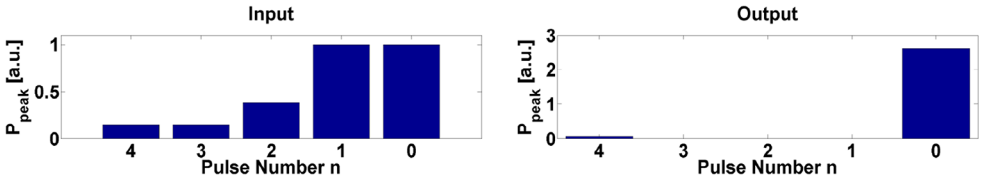

Fig. 14. The simulated input and output pulse peak power amplitudes for a single GTI cavity.

the last two input pulses have the same amplitude, which corresponds to the optimum pulse energy enhancement factor. In addition, to achieve perfect destructive and constructive interferences on the partially-reflecting cavity front mirror, when the cavity round-trip length is stabilized to integer numbers of the optical pulse carrier wavelength, all the pulses in an input pulse burst have uniform phases except that the very last pulse has a phase offset of π. This phase offset is for the final constructive interference on the cavity front mirror to extract all the stored energy in the GTI cavity.

Here we experimentally demonstrate single-cavity coherent stacking of a 5-pulse burst of femtosecond pulses into a solitary stacked pulse with a pulse energy up to 100 μJ. The input burst of pulses is from a 55 μm chirally-coupled-core (CCC) fiber amplifier based MOPA system.

The complete experimental setup is shown in Fig. 15. A mode-locked laser outputs a 122 MHz pulse sequence at 1054 nm central wavelength, which is subsequently stretched by a grating stretcher and coupled into a polarization-maintaining single-mode fiber and divided by a splitter into two separate fiber channels, stacking channel and monitor channel respectively. The monitor signal is phase modulated and used for stabilizing the GTI cavity length. For coherent pulse stacking the GTI resonator length has to be precisely controlled using a PZT mirror. In the stacking channel amplitude- and phase-tailored pulse bursts are produced by imprinting the required amplitude and phase modulation/code with the amplitude modulator and the phase modulator. The pulse bursts are then sent through a series of three pre-amplifiers with acousto-optic modulators (AOM) to down-count the repetition rate to 80 kHz. The amplified bursts then go through a co-pumped monolithic amplifier stage based on 25 μm LMA, followed by a counter-pumped 55 μm CCC based amplifier stage. The pulse burst is boosted to a burst energy of up to 100 uJ at an average power of 8 W. The amplified signal and the monitor signal share the GTI cavity by polarization multiplexing. A Herriott cell is incorporated inside the GTI cavity to fold 2.4 m of total GTI roundtrip length into only a 12 cm mirror separation, with the beam undergoing 10 roundtrips between the two Herriott cell mirrors. This very compact

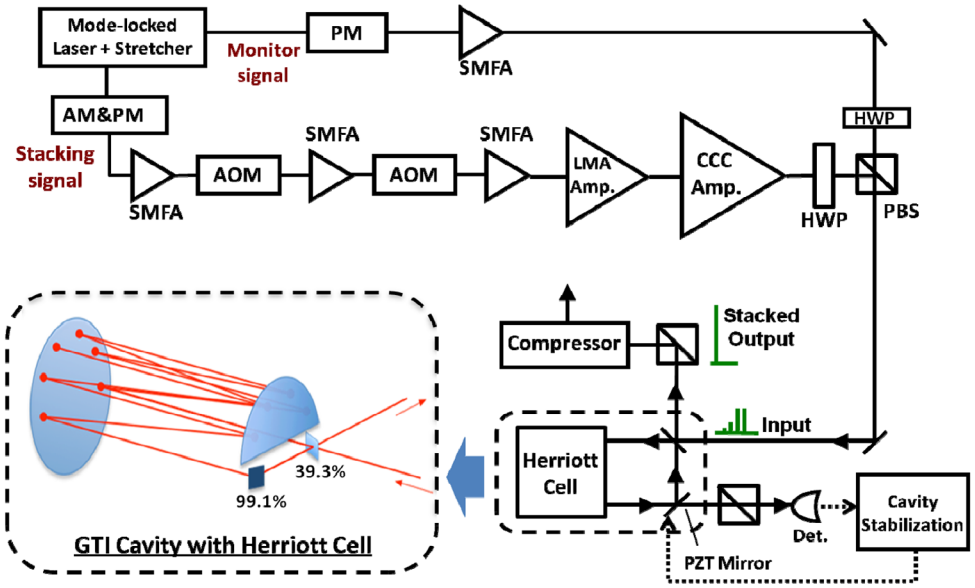

Fig. 15. Experimental CPSA setup. AM&PM: amplitude&phase modulators; SMFA: single-mode fiber amplifier; AOM: acousto-optic modulator; LMA Amp.: large-mode-area fiber amplifier; CCC Amp.: chirally-coupled-core fiber amplifier; HWP: half-wave plate; Det.: detector.

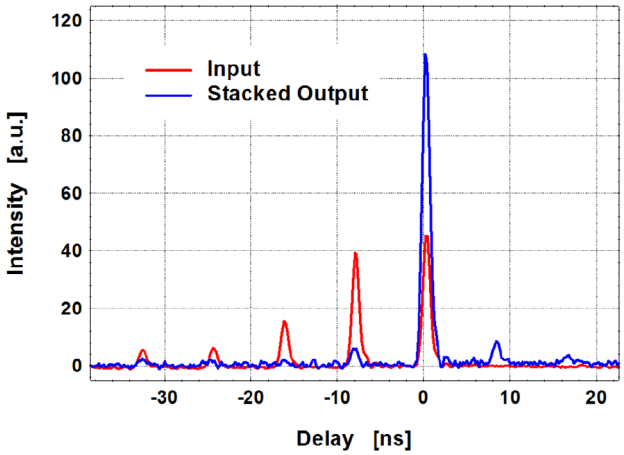

Fig. 16. The input pulse burst and the output stacked pulse of a single GTI cavity.

cavity folding technique is of critical importance for stacking large numbers of pulses, which will be discussed in Subsection 3.3. Finally, the stretched chirped pulses in an amplified pulse burst are coherently stacked into a solitary output chirped pulse by the GTI cavity.

The input pulse burst to the GTI cavity and the output stacked pulse with a pulse energy of 12.5 μJ are shown in Fig. 16. The pulse energy enhancement factor is measured to be 2.4 and the pre-pulse contrast, which is defined as the pulse energy ratio between the output stacked pulse and its pre-pulse, is measured to be 13 dB.

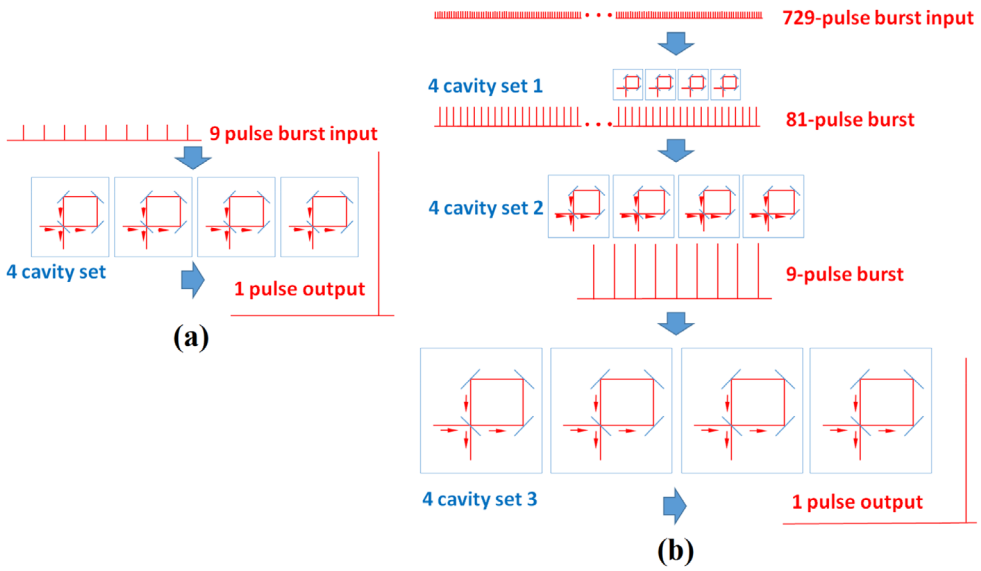

Fig. 17. (a) 4 cascaded equal roundtrip GTI cavities; (b) 3 sets of 4 cascaded GTI cavities with different cavity roundtrips for each set.

3.3 CPSA of large number of pulses by cascading and multiplexing GTI cavities

CPSA based on a single GTI cavity can only have a maximum possible pulse energy enhancement factor of ~2.5, which is shown previously. However, coherent stacking of large numbers of equal-amplitude pulses and thus much larger pulse energy enhancement factors can be achieved by using properly configured sequences of multiple GTI cavities, as illustrated in Fig. 17. Here a burst of input pulses are "carved out" directly from a periodic pulse train from a mode-locked oscillator, then properly amplitude/phase modulated and amplified, thus when entering a set of cascaded GTI cavities they destructively interfere at the partially-reflecting front mirror of the final GTI, until the final input pulse in a burst constructively interferes with the intracavity pulses of all the GTIs at their partially-reflecting front mirrors, thus extracting all the stored energy from the cavities into a single output pulse. Assuming coherent stacking here is lossless and linear, the process obeys time reversal symmetry so that it can be considered as the reversed process of inputting a single pulse into a set of cascaded GTI cavities and getting a sequence of output pulses whose amplitudes and phases are functions of the cavity front mirror reflectivities and the cavity phases (lengths). As a result, the cavity parameters can be properly chosen so that in a coherent stacking process the input burst has near equal-amplitude pulses which can be coherently stacked into a solitary output pulse, and thus the pulse energy enhancement factor is maximized.

Considering a cascaded sequence of N equal-roundtrip GTI cavities, it can be shown mathematically that when an incident burst of pulses produces a single output stacked pulse, the amplitude of each pulse in the input burst is a function of the N GTI front mirror reflectivities and N GTI round-trip phases. Thus mathematically, by properly adjusting the 2N-1 independent cavity parameters, the pulse energies of the last 2N pulses in the input burst can be set equal, which results in a pulse energy enhancement factor of >2N. Note here 2N-1 independent cavity parameters are all N GTI front mirror reflectivities and N-1 GTI round-trip phases,

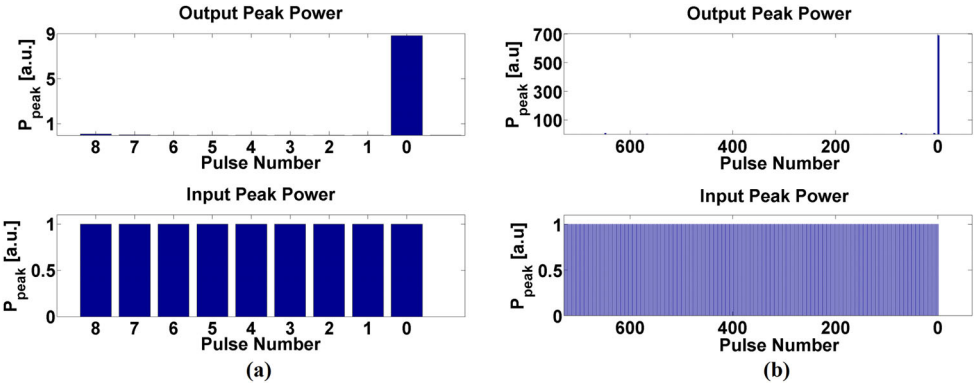

Fig. 18. (a) The input and output pulse peak power amplitudes for 4 cascaded GTI cavities; (b) The input and output pulse peak power amplitudes for 3 sets of 4 cascaded GTI cavities.

since one of the N round-trip phases can be freely selected, which only affects the required individual pulse phases of the input pulse burst. A CPSA simulation based on four cascaded equal-roundtrip GTI cavities is presented in Fig. 18(a), showing an input pulse sequence consisting of 9 equal-amplitude pulses and an output stacked pulse with a numerical pulse energy enhancement factor of $\eta = 8.8$. Here the GTI front mirror reflectivies and cavity round-trip phases are set as follows: $R_1 = 0.535$, $R_2 = 0.516$, $R_3 = 0.618$, $R_4 = 0.666$, $\delta_1 = 4.66$, $\delta_2 = 3.15$, $\delta_3 = 5.46$, and we let $\delta_4 = 0$.

Since when cascading equal-roundtrip GTI cavities, the enhancement factor grows linearly with the number of cavities, large enhancement factors require large numbers of cavities, which is of limited practicality. The solution is to cascade sets of cavities, where each set of cavities has a different specified roundtrip length. For example, when cascading two sets of cavities, the second set of cavities will have a roundtrip length that is at least 2N times larger than the first set, where N is the number of cavities in the first set. In this case, the output stacked pulse sequence of the initial set of N cascaded equal-roundtrip GTI cavities can be used as the input signal of the subsequent set of N cascaded equal-roundtrip GTI cavities. Assuming the pulse energy enhancement factor of the first set of cascaded GTIs is η, then the total pulse energy enhancement factor would be η^2 for the two sets of cascaded GTIs. Therefore when cascading M sets of N cascaded GTI cavities, the total pulse energy enhancement for the full configuration will be η^M. Using multiple sets of different length cascaded cavities is what allows this technique to be suitable for generating very large energy pulses (>10 J) from a small number of parallel channels as well as only a few cavities. For example, starting with a high repetition rate oscillator (1 GHz), and using 3 sets of 4 GTI cavities with roundtrip lengths of 0.3 m, 2.7 m, and 24.3 m respectively will allow 729 equal-amplitude input pulses to be stacked into an output pulse with a pulse energy enhancement of $\eta \approx 8.8^3 \approx 681$. Figure 18(b) is a numerical simulation of this case where front mirror reflectivities and cavity roundtrip phases for each set are the same as those for the cascaded four GTIs case. Therefore, starting with relatively low input pulse energies gives the ability to extract all of the stored energy from a single fiber amplifier with low nonlinearity.

In order to achieve very large stacking enhancement factors, GTI cavities with long roundtrip lengths are needed in order to satisfy the 2N scaling condition on the subsequent sets (as seen from the previous example with cavities that have a 24.3 m roundtrip length). Thus it is greatly beneficial to use multi-pass Herriott-type cells to provide long cavity lengths with small footprints. This Herriott cell inside the

GTI cavity serves as a very compact and q-parameter preserving folded delay line, as shown in Sect. 3.2. For the other example of the 3 sets of 4 GTI cavities with roundtrip lengths of 0.3 m, 2.7 m, and 24.3 m it is possible to use Herriott cells to compactly fold the 2.7 m cavities into roughly 10 cm mirror separations, and the 24.3 m cavities into roughly 50 cm mirror separations. This will allow all of the cavities to be folded into a compact arrangement, thus making the technique very practical.

4 Summary

In this paper we conceptually introduce and demonstrate experimentally two new time-domain pulse multiplexing and beam combining techniques, which can lead to orders of magnitude reduction in the coherently combined fiber amplifier array size for achieving very high energy (in the range 1–10 J) ultrashort pulses compatible with 10 GeV energy laser plasma acceleration of electrons. Both techniques achieve coherent pulse stacking using resonant optical cavities. It is important to note that the round-trip length of stacking cavities should match repetition period between the pulses that are being stacked, not the resulting "stacked" pulse train repetition period. This is due to causality constraint only requiring that pulse stacker response time cannot be shorter than temporal separation between adjacent pulses in the incident train. Therefore, when starting with a high repetition rate pulse train from a mode locked laser such stacking/combining cavities can be made very compact, particularly when using Herriott cell folding.

At this point it is worth commenting that, while both presented techniques provide with useful avenues of increasing pulse energy per parallel amplification channel, it is the CPSA technique that is much better suited for significantly reducing fiber array size of the envisioned 10 GeV laser-plasma accelerator drivers. Indeed, use of the N^2 technique is constrained by its applicability only to strictly periodic pulse trains. This leads to a certain trade-off, which can be highlighted by a particular example. Let's consider a 1 MHz repetition rate incident pulse train. The corresponding combiner round-trip length is 300 m. Let's assume that using Herriott cell this cavity can be folded hundreds times, into approximately 3 m long folded setup. This is feasible with existing state of the art dielectric mirror coatings. Implementation of N^2 scheme with 10 channels would reduce the repetition rate down to 100 kHz, and would increase pulse energy by 100 times. Assuming 1 mJ per pulse in the incident pulse train (1 kW average power) one would obtain 100 mJ per pulse in the combined beam, with the corresponding average power at the output of 10 kW. Implementation of N^2 scheme with 100 channels would reduce the repetition rate down to 10 kHz, and would increase pulse energy by 10^4 times reaching up to 10 J, with the total combined average power of 100 kW. However, this would be achieved at the expense of a rather complex and large beam combining/pulse stacking arrangement.

In contrast, CPSA technique can be applied to equal-amplitude pulse bursts, where these bursts are produced at any arbitrary repetition rate (including a single shot operation). Consequentially, as it was shown earlier, a relatively small number of GTI-based pulse stackers ($\sim$10–15) is sufficient to achieve pulse stacking factors between 100 and 1000. Of course, in this case extractable pulse energy per channel is limited by the stored energy in a fiber, which for large-core state-of-the-art fibers reaches into 10 mJ to 50 mJ range. As a result of such high stacking factors it is possible to generate >10 J pulses with array sizes as small as 100 to 1000 parallel channels, and with each individual pulse energy in a single-channel stacking burst $<100\,\mu$J, producing very low B-integral values and, therefore, negligible pulse distortions.

References

1. D. Strickland, G. Mourou, Opt. Commun. **55**, 447 (1985)
2. F. Röser, T. Eidam, J. Rothhardt, O. Schmidt, D.N. Schimpf, J. Limpert, A. Tünnermann, Opt. Lett. **32**, 3495 (2007)
3. W. Leemans, E. Esarey, Phys. Today **62**, 44 (2009)
4. M. Kienel, A. Klenke, T. Eidam, S. Hädrich, J. Limpert, A. Tünnermann, Opt. Lett. **39**, 1049 (2014)
5. Y. Zaouter, F. Guichard, L. Daniault, M. Hanna, F. Morin, C. Hönninger, E. Mottay, F. Druon, P. Georges, Opt. Lett. **38**, 106 (2013)
6. R.J. Jones, J. Ye, Opt. Lett. **27**, 1848 (2002)
7. S. Breitkopf, T. Eidam, A. Klenke, L. von Grafenstein, H. Carstens, S. Holzberger, J. Limpert, Light: Sci. Appl. **3**, e211 (2014)
8. T. Zhou, J. Ruppe, C. Zhu, I. Hu, J. Nees, A. Galvanauskas, Coherent Pulse Stacking Amplification of Nanosecond and Femtosecond Pulses. In *Advanced Solid State Lasers (ASSL2014)* (Shanghai, China, 2014), p. AW4A-7
9. L.A. Siiman, W.Z. Chang, T. Zhou, A. Galvanauskas, Opt. Expr. **20**, 18097 (2012)